Central Bouquet Hemorrhages in Retinal Vein Occlusion: A Distinct Pathway to Macular Atrophy

Maria Vittoria Cicinelli,[1,2] Enrico Maria Pepe,[1] Prithvi Ramtohul,[3] Beatrice Tombolini,[4] Stefano Puligheddu,[1,2] Alessandro Russo,[1] Francesco Bandello,[1,2] and Rosangela Lattanzio[1,2]

[1]School of Medicine, Vita-Salute San Raffaele University, Milan, Italy
[2]Department of Ophthalmology, IRCCS San Raffaele Scientific Institute, Milan, Italy
[3]Ophthalmology Department, Hôpital Nord, Aix-Marseille University, Marseille, France
[4]Department of Ophthalmology, Circolo Hospital and Macchi Foundation, Varese, Italy

Correspondence: Maria Vittoria Cicinelli, Department of Ophthalmology, IRCCS San Raffaele Scientific Institute, Via Olgettina 60, Milan 20132, Italy; Cicinelli.mariavittoria@hsr.it.

Received: June 16, 2025
Accepted: August 27, 2025
Published: September 26, 2025

Citation: Cicinelli MV, Pepe EM, Ramtohul P, et al. Central bouquet hemorrhages in retinal vein occlusion: A distinct pathway to macular atrophy. *Invest Ophthalmol Vis Sci*. 2025;66(12):62. https://doi.org/10.1167/iovs.66.12.62

Purpose. To characterize central bouquet hemorrhages (CBHs) in retinal vein occlusion (RVO) and evaluate their association with long-term visual and anatomical outcomes, in particular macular atrophy. This is a retrospective longitudinal cohort study of 403 treatment-naïve eyes with RVO (mean age, 62.9 ± 15.4 years; 59% male).

Methods. CBH was identified on spectral-domain optical coherence tomography as vertically oriented light-absorbing masses centered at the fovea, above the external limiting membrane. Clinical characteristics, imaging findings, and intravitreal treatment frequency were compared between eyes with and without CBH. Baseline and longitudinal visual acuity analyzed with multivariable regression models, the prevalence of CBH-related features, and the cumulative incidence and predictors of macular atrophy assessed with Cox regression models were assessed.

Results. CBH were observed in 28% of eyes (n = 111) at baseline. Affected eyes were older, had more systemic vascular comorbidities, and presented with more severe macular edema, peripapillary hemorrhages, and cotton-wool spots (all $P < 0.001$). Ischemic markers—including arteriolar paracentral acute middle maculopathy ($P = 0.04$) and increased ischemic index on fluorescein angiography ($P = 0.02$)—were more common in CBH eyes. Over time, CBH reabsorbed, often leaving a plaque-like RPE thickening, which progressed to outer retinal atrophy in 69% of cases over 36 months. Severe cystoid macular edema and full-thickness macular holes were also common. CBH was independently associated with worse baseline visual acuity ($\beta = 0.09$ logMAR; 95% confidence interval [CI], 0.01–0.18; $P = 0.04$) and slower visual recovery (β for CBH × Time = −0.002 logMAR/month; $P < 0.001$). Intravitreal treatments reduced the risk of macular atrophy (hazard ratio, 0.28; 95% CI, 0.08–0.96; $P = 0.04$), and each additional injection conferred a protective effect (hazard ratio, 0.96; 95% CI, 0.93–0.99; $P = 0.02$).

Conclusions. CBH represents a characteristic hemorrhagic manifestation in RVO, likely reflecting the localized effects of elevated venous pressure and macular ischemia that contribute to structural disruption and poor visual outcomes. Its presence warrants close monitoring and sustained treatment to mitigate long-term retinal damage.

Keywords: retinal vein occlusion, central cone bouquet, macular hemorrhages, Henle fiber layer, RPE atrophy

Retinal vein occlusion (RVO) is a leading cause of vision loss worldwide and represents the second most prevalent retinal vascular disorder after diabetic retinopathy.[1] Depending on the anatomical site of occlusion, RVO is classified into central (CRVO), branch, or hemiretinal subtypes, each with distinct clinical features. Despite these differences, all forms share a common pathophysiological mechanism of venous outflow obstruction, resulting in retinal ischemia, macular edema, and hemorrhage.[2]

Intraretinal hemorrhages are a hallmark of RVO and serve as both a diagnostic clue and a prognostic indicator; they often mirror the severity and distribution of vascular compromise. In the early stages, bleeding typically involves the intermediate capillary plexus and deep capillary plexus (DCP), with subsequent extension to the superficial capillary plexus and radial peripapillary capillaries in more advanced stages of the disease.[3] Flame-shaped hemorrhages along the retinal nerve fiber layer (RNFL) have been associated with greater ischemia, increased macular edema, and poorer visual outcomes.[4]

Beyond the RNFL, hemorrhages may also affect Henle's fiber layer (HFL), the obliquely oriented axonal zone of

cone photoreceptors, and have been associated with selective DCP damage.[5,6] A distinct morphological variant of HFL hemorrhage—termed *central bouquet hemorrhage* (CBH)—has been described on optical coherence tomography (OCT), corresponding with hemorrhage within the cone bouquet, a specialized zone containing densely packed cone axons and Müller cells.[7,8] CBH is often associated with delayed resorption, persistent disruption of the ellipsoid zone, and localized outer retinal atrophy, suggesting that it may contribute to photoreceptor damage and long-term visual loss.[9]

Despite its recognition in other retinal pathologies,[9] CBH has not been systematically investigated in RVO. Given the shared vascular stressors—including venous hypertension and DCP involvement—it is plausible that CBH occurs in RVO more frequently than previously appreciated, yet remains underdiagnosed. In this study, we analyzed a large cohort of treatment-naïve eyes with acute RVO to evaluate the prevalence, imaging features, and clinical relevance of CBH. We characterized its morphology on multimodal imaging, described its longitudinal evolution, and assessed its association with visual and anatomical outcomes. Our findings suggest that CBH represents a distinct hemorrhagic phenotype in RVO with prognostic significance, particularly as a potential mediator of macular atrophy.

Methods

This retrospective cohort study included patients newly diagnosed with treatment-naïve RVO who presented to the Medical Retina Unit of the Department of Ophthalmology, IRCCS Ospedale San Raffaele (Milan, Italy) between January 2011 and April 2025. The study followed the principles of the Declaration of Helsinki and was approved by the Institutional Review Board, which waived the need for written informed consent owing to the study's retrospective nature.

Participants were eligible if they met the following criteria: (1) age 18 years or older, (2) RVO diagnosis confirmed through multimodal imaging, (3) symptom onset within 3 months of presentation, and (4) at least one baseline spectral-domain OCT (SD-OCT) volume scan available. Patients were excluded if they had (1) other maculopathy-inducing retinal or optic nerve diseases (e.g., diabetic macular edema, neovascular AMD, pseudophakic cystoid macular edema), (2) significant media opacities preventing adequate imaging, (3) previous macular edema treatments (anti-VEGF, laser, or steroids), or (4) intraocular surgery within the preceding 6 months. Although all eyes were treatment naïve at baseline, intravitreal therapy was not a mandatory inclusion criterion.

Baseline systemic information included patient age, sex, and self-reported history of hypertension, diabetes mellitus, dyslipidemia, cardiovascular events (e.g., myocardial infarction, angina, stroke), inflammatory or hematological disorders, and glaucoma, extracted from electronic medical charts (nLIFE, NIDEK Technologies, Padova, Italy). Start and end dates of follow-up were recorded for longitudinal analyses.

All patients underwent a full ophthalmic evaluation at each visit, including best-corrected visual acuity (VA, measured with the Early Treatment Diabetic Retinopathy Study charts), slit-lamp examination, and dilated ophthalmoscopy. VA was converted to the logMAR scale; counting fingers and hand motion vision were assigned a logMAR of 1.5 and 2.0, respectively.

Multimodal Imaging and Hemorrhage Classification

Baseline imaging included ultra-widefield color photography (Optos, Dunfermline, UK) and SD-OCT (Spectralis HRA+OCT, Heidelberg Engineering, Heidelberg, Germany), comprising both a 19-line horizontal raster and a high-density 46-line macular volume scan. When available, fundus autofluorescence and fluorescein angiography (FA) were also reviewed. RVO subtype (CRVO, branch RVO, or hemiretinal RVO) was determined based on imaging findings and clinical documentation.

Hemorrhages were categorized by location and depth using color fundus photography, FA, and OCT. RNFL hemorrhages were defined as flame-shaped lesions aligned with nerve fiber bundles.[4] Deep hemorrhages were located beneath the superficial vascular plexus and appeared rounded. Henle fiber layer hemorrhages were identified based on their radial or petaloid configuration on fundus images and oblique hyper-reflective bands with hyporeflective septa on OCT.[5]

Central bouquet hemorrhages were defined primarily on OCT as vertically oriented, hyper-reflective intraretinal light absorbing masses situated above or within the outer nuclear layer (ONL), typically confined to the central foveal region corresponding to the cone bouquet within the HFL. These lesions varied from compact and ovoid to fragmented and multilobular, depending on surrounding edema.[10] In all cases, infrared reflectance imaging co-registered with OCT line scans was used to precisely the foveal center localize and confirm the presence and extent of CBH. This multimodal approach, as shown previsouly,[5,11] enhances the detection and characterization of fovea-involving hemorrhage, particularly when hemorrhages are not clearly visible on fundus photography

SD-OCT Analysis

Center-involving macular edema was diagnosed based on cystoid changes on SD-OCT. Fluid compartments were classified as inner (anterior to the ONL), outer (within the ONL), or RNFL involving. The presence of subretinal fluid was also recorded. Central macular thickness (CMT) was extracted using automated segmentation from the 1-mm Early Treatment Diabetic Retinopathy Study central subfield.

The integrity of inner and outer retinal layers—including the ellipsoid zone and RPE—was assessed on follow-up scans. Disorganization of the retinal inner layers (DRIL) was defined as the loss of identifiable boundaries between the ganglion cell–inner plexiform layer complex, inner nuclear layer, and outer plexiform layer in the central fovea.[12] Macular atrophy was defined by the presence of all of the following: (1) choroidal hypertransmission, (2) RPE loss or attenuation, and (3) overlying photoreceptor degeneration.[13] Lesions were documented regardless of minimum size criteria.

Ischemia-associated OCT features were also analyzed, including: (1) inner retinal thickening with RNFL hyperreflectivity (indicative of superficial ischemia),[14] (2) paracentral acute middle maculopathy (PAMM), characterized by hyper-reflective bands in the inner nuclear layer, and (3) the prominent middle limiting membrane sign, appearing as a hyper-reflective band at the inner border of the outer plexiform layer.[15] PAMM lesions were subclassified as arteriolar

(linear), globular (focal), or fern like (multilobulated with venular distribution).[16]

Quantitative FA Analysis

In eyes with available ultra-widefield FA, the clearest image acquired during the early arteriovenous phase (45–60 seconds post injection) was selected for analysis.[17] The image with the widest retinal coverage was exported at 1.86× magnification. A trained grader (E.P.), masked to clinical data, manually outlined the total visible retina and nonperfused areas using ImageJ software. The ischemic index was computed as the ratio of nonperfusion to total retinal area, according to validated protocols.

Treatment Protocol

Eyes with macular edema received either intravitreal anti-VEGF agents (ranibizumab or aflibercept 2.0 mg) or dexamethasone implants, based on the treating physician's discretion. Steroids were preferred in cases of cardiovascular comorbidities, pseudophakia, or expected poor treatment adherence. In eyes with CBH, we recorded the interval between the RVO diagnosis and the first injection, as well as the total number of intravitreal injections administered during follow-up, to assess the relationship between treatment frequency, timing, and structural outcomes.

Statistical Analyses

All statistical analyses were conducted using R software (R Core Team, Vienna, Austria). All tests were two sided, and a P value of less than 0.05 was considered statistically significant. Quantitative variables were summarized as mean ± SD, and categorical variables were presented as absolute frequencies and percentages. Demographic and clinical differences between eyes with and without CBH were evaluated using linear regression for continuous variables and logistic regression for categorical variables.

Baseline VA was analyzed using a multivariable linear regression model. A predefined set of clinically relevant predictors was selected, including CBH status, demographic characteristics (age, sex), RVO subtype, and OCT imaging biomarkers. Missing data were addressed using multiple imputations by chained equations with predictive mean matching. Stepwise variable selection based on the Akaike information criterion was applied to identify the most parsimonious model. Model diagnostics included residual analysis to assess linearity and homoscedasticity, variance inflation factors to check for multicollinearity, and Cook's distance to identify influential observations. Model performance was evaluated using the adjusted coefficient of determination (adjusted R^2).

To investigate changes in VA over time and their association with CBH, a linear mixed-effects model was fitted, with VA as the dependent variable. Fixed effects included CBH status, follow-up time from occlusion (in months), and their interaction. A random intercept was specified for each eye to account for repeated measurements. The significance of the interaction term was used to test whether CBH modified the trajectory of VA during follow-up.

Finally, the cumulative incidence of RPE atrophy in eyes with CBH was estimated using Kaplan–Meier survival analysis. Eyes without RPE atrophy were censored at the last available follow-up. To identify predictors of RPE atrophy development, univariable Cox proportional hazards regression models were constructed, and hazard ratios (HRs) were provided.

Results

A total of 403 treatment-naïve eyes with RVO were included (mean age, 62.9 ± 15.4 years; 59% males), of which 111 eyes (28%) exhibited CBH. Eyes with CBH belonged to significantly older patients (68.3 ± 11.6 years vs. 60.8 ± 16.2 years; $P < 0.001$), whereas the proportion of males was similar between groups (60% vs. 59%).

Eyes with CBH were associated with a higher burden of systemic comorbidities (Table 1). Their corresponding patients more frequently had hypertension (71% vs. 52%; $P < 0.001$) and cardiovascular disease (36% vs. 18%; $P < 0.001$). Glaucoma was also more common in eyes with CBH (25% vs. 14%; $P = 0.01$). Conversely, diabetes ($P = 0.2$) and dyslipidemia ($P = 0.5$) rates were comparable, and hematological disorders were less frequent (7% vs. 14%; $P = 0.04$).

Qualitative Description

Central bouquet hemorrhages appeared as deep, centrally located red foveal hemorrhages on color fundus photography and exhibited distinctive morphological features on OCT. Typically, CBH presented as vertically oriented, ovoid or piriform light absorbing masses situated immediately above the external limiting membrane (Fig. 1). When compact, these lesions cast dense posterior shadowing that obscured the visualization of deeper retinal layers. In some cases, a linear extension from the hemorrhagic core was observed, suggestive of blood tracking obliquely along Henle fiber trajectories (Fig. 1B). In all cases, CBH corresponded with hyporeflective lesions on infrared reflectance imaging, and co-registration with OCT line scans allowed precise localization of the foveal center and confirmation of CBH extent. Supplementary Figures S1 and S2 illustrate representative examples of this multimodal approach.

In eyes with prominent ONL edema, the rounded contour of CBH evolved into a vertically elongated or linear configuration (Figs. 1D and 1F). Less compact or more dispersed hemorrhages appeared as fragmented or punctate hyperreflective fragments within the edematous ONL, consistent with intraretinal blood dispersion. This dispersion was particularly evident in the presence of large central cystoid spaces, where blood infiltrated the cyst lumen, forming layered or whorled patterns resembling dye diffusing in liquid (Fig. 1B). When CBH coexisted with subretinal hemorrhage (64%), it occasionally formed a continuous anatomical complex spanning both compartments (Fig. 1B).

On en face OCT, available in a subset of eyes with CBH, the hemorrhage appeared as a centrally located hyperreflective foveal lesion on reconstructions at the level of the Henle fiber layer and ONL. In some eyes, surrounding or overlying round hyporeflective spaces were also observed, corresponding with cystoid edema.

RVO Characteristics in CBH Eyes

Eyes with CBH had a similar distribution of RVO subtypes compared with those without CBH, with CRVO being the most frequent in both groups (53% vs. 57%; $P = 0.8$). However, macular edema was significantly more common

Table 1. Demographic, Systemic, and Ocular Baseline Characteristics of Eyes With and Without CBH at Presentation

	CBH (n = 111 Eyes)	No CBH (n = 292 Eyes)	Overall (n = 403 Eyes)
Age (years)	68.3 ± 11.6	60.8 ± 16.2	62.9 ± 15.4
Male sex	66 (59.5)	171 (58.6)	237 (58.8)
Hypertension	79 (71.2)	151 (51.7)	230 (57.1)
Missing	1 (0.9)	7 (2.4)	8 (2.0)
Diabetes	19 (17.1)	36 (12.3)	55 (13.6)
Missing	1 (0.9)	6 (2.1)	7 (1.7)
Cardiovascular diseases	40 (36.0)	53 (18.2)	93 (23.1)
Missing	1 (0.9)	7 (2.4)	8 (2.0)
Dyslipidemia	28 (25.2)	84 (28.8)	112 (27.8)
Missing	2 (1.8)	6 (2.1)	8 (2.0)
Hematologic disorders			
No abnormality detected	103 (92.8)	250 (85.6)	353 (87.6)
Autoimmune condition	0 (0)	6 (2.1)	6 (1.5)
Vitamin deficiency	1 (0.9)	0 (0)	1 (0.2)
Thrombophilia	5 (4.5)	23 (7.9)	28 (6.9)
Blood dyscrasia	1 (0.9)	6 (2.1)	7 (1.7)
Missing	1 (0.9)	7 (2.4)	8 (2.0)
Inflammatory conditions	2 (1.8)	7 (2.4)	9 (2.2)
Glaucoma	28 (25.2)	42 (14.4)	70 (17.4)
VA (logMAR)	0.808 ± 0.485	0.382 ± 0.406	0.497 ± 0.468
Macular edema at baseline	106 (95.5)	226 (77.4)	332 (82.4)
Type RVO			
CRVO	59 (53.2)	167 (57.2)	226 (56.1)
HRVO	17 (15.3)	35 (12.0)	52 (12.9)
BRVO	35 (31.5)	90 (30.8)	125 (31.0)
CMT (micron)	777 (261)	501 (218)	577 (261)
Outer fluid	104 (93.7)	217 (74.3)	321 (79.7)
Inner fluid	90 (81.1)	169 (57.9)	259 (64.3)
RNFL fluid	35 (31.5)	28 (9.6)	63 (15.6)
SRF	97 (87.4)	151 (51.7)	248 (61.5)
PAMM	19 (17.1)	50 (17.1)	69 (17.1)
Arteriolar	11 (9.9)	12 (4.1)	23 (5.7)
Fern-like	6 (5.4)	25 (8.6)	31 (7.7)
Globular	2 (1.8)	13 (4.5)	15 (3.7)
p-MLM sign	84 (75.7)	139 (47.6)	223 (55.3)
RNFL hyper-reflectivity	67 (60.4)	83 (28.4)	150 (37.2)
Ischemic index (%)	27.5 ± 16.6	20.0 ± 14.7	22.3 ± 15.5
Missing	62 (55.9)	183 (62.7)	245 (60.8)
Cotton wool spots	63 (56.8)	102 (34.9)	165 (40.9)
Deep hemorrhages	109 (98.2)	279 (95.5)	388 (96.3)
RNFL hemorrhages	83 (74.8)	180 (61.6)	263 (65.3)
HFL hemorrhages	74 (66.7)	67 (22.9)	141 (35.0)

BRVO, branch retinal vein occlusion; CRVO, central retinal vein occlusion; HFL, Henle fiber layer; HRVO, hemiretinal vein occlusion; p-MLM, prominent middle limiting membrane; SRF, subretinal fluid.

Data are presented as number (percentage) for categorical variables, and as mean ± SD for continuous variables.

in eyes with CBH (96% vs. 77%; $P < 0.001$), and these eyes exhibited markedly greater CMTs (777 ± 261 µm vs. 501 ± 218 µm; $P < 0.001$). Among eyes with edema, those with CBH more frequently showed inner retinal edema (81% vs. 58%; $P = 0.04$), RNFL edema (32% vs. 10%; $P < 0.001$), and subretinal fluid (87% vs. 52%; $P < 0.001$).

Fundus examination revealed similarly high frequencies of deep retinal hemorrhages (98% vs. 96%; $P = 0.3$), but RNFL peripapillary hemorrhages were significantly more common in eyes with CBH (75% vs. 62%; $P = 0.01$). Henle fiber layer hemorrhages were also more prevalent (67% vs. 23%; $P < 0.001$), as were cotton wool spots (57% vs. 35%; $P < 0.001$).

OCT imaging showed that ischemic structural markers were more common in the CBH group. These eyes more often had RNFL hyper-reflectivity (60% vs. 28%; $P < 0.001$) and a positive prominent middle limiting membrane sign (76% vs. 48%; $P < 0.001$). Although the overall prevalence of PAMM did not differ (17% vs. 17%; $P = 0.9$), arteriolar PAMM was significantly more common in eyes with CBH (10% vs. 4%; $P = 0.04$). FA supported these findings, revealing a significantly higher ischemic index in CBH eyes (28 ± 17% vs. 20 ± 15%; $P = 0.02$).

Evolution of CBH Over Time

Eyes with CBH demonstrated gradual reabsorption of the hemorrhage over time. In many cases (42%), this process left behind a vertically oriented hyper-reflective linear remnant spanning the foveal axis (Fig. 2D). Disruption of the outer retinal layers—specifically the ellipsoid zone and external limiting membrane—persisted at the original site of the hemorrhage in 85% of eyes (Figs. 2E and 3).

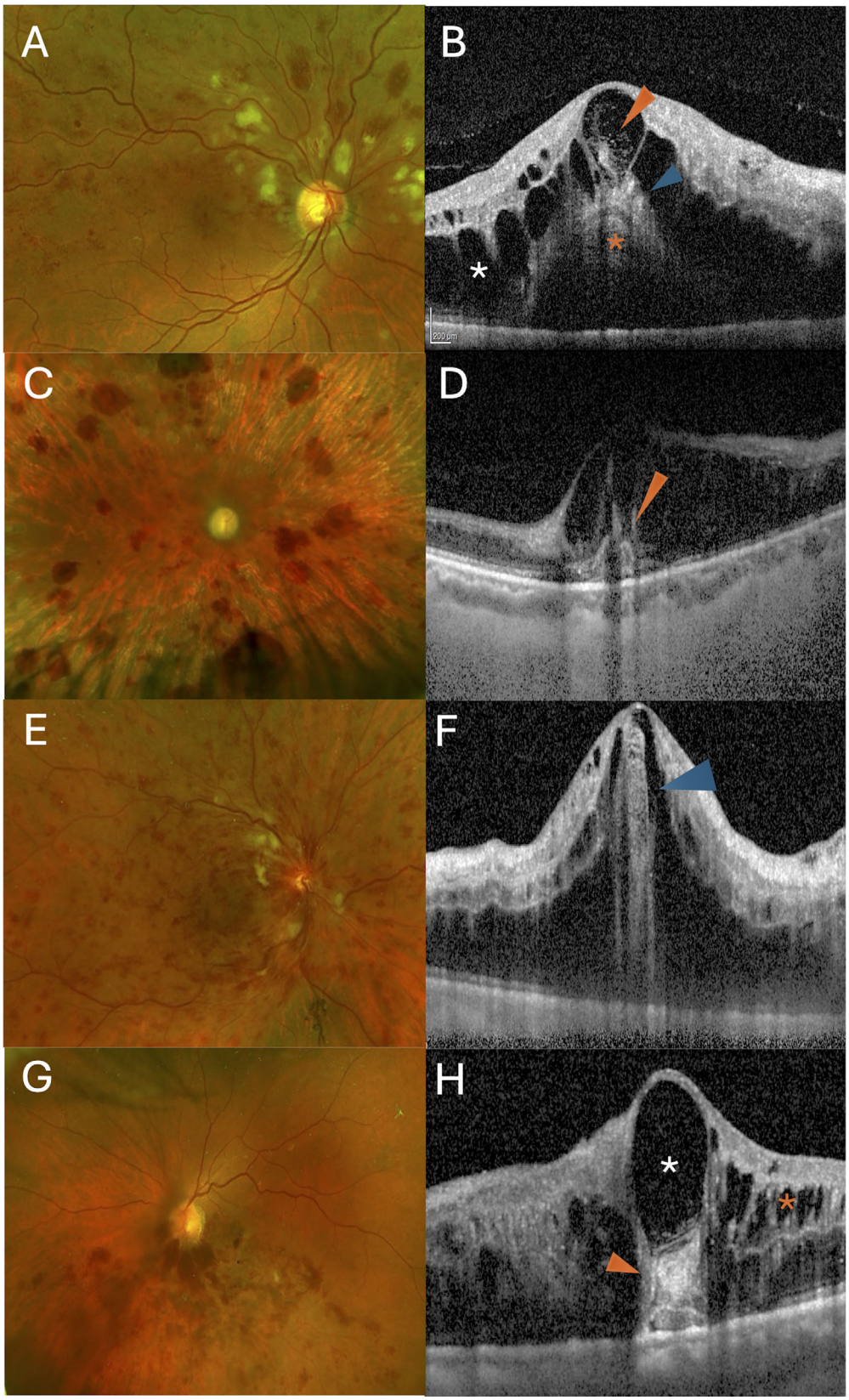

Figure 1. Multimodal imaging of CBHs in RVO. Ultra-widefield pseudocolor fundus photographs (left column) and corresponding SD-OCT scans (*right*) from four treatment-naïve patients with acute RVO. (**A**, **B**) A man in his 70s with superior hemi-RVO. OCT reveals ONL edema (*white asterisk*) and a large central cystoid cavity containing hemorrhagic material with a layered, whorled appearance (*orange arrowhead*). A compact hyper-reflective lesion is seen between the cyst and the external limiting membrane (ELM), consistent with CBH (*blue arrowhead*). Subretinal hyper-reflective dots suggest concurrent subretinal hemorrhage (*orange asterisk*). (**C**, **D**) A man in his 60s with CRVO. OCT shows vertically oriented, sharply delineated hyper-reflective lesions above the ELM, casting posterior shadowing—hallmark features of CBH (*orange arrowhead*). (**E**, **F**) A woman in her 60s with CRVO. OCT reveals a vertically aligned CBH extending from the ELM

Investigative Ophthalmology & Visual Science

through the ONL (*blue arrowhead*), embedded within the edematous retina and exhibiting a dome-shaped upper contour. (**G**, **H**) A man in his 70s with inferior hemi-RVO. OCT displays widespread intraretinal fluid (*orange asterisk*), a central ONL cyst (*white asterisk*), and a compact hyper-reflective lesion with squared contours above the ELM, characteristic of CBH (*orange arrowhead*).

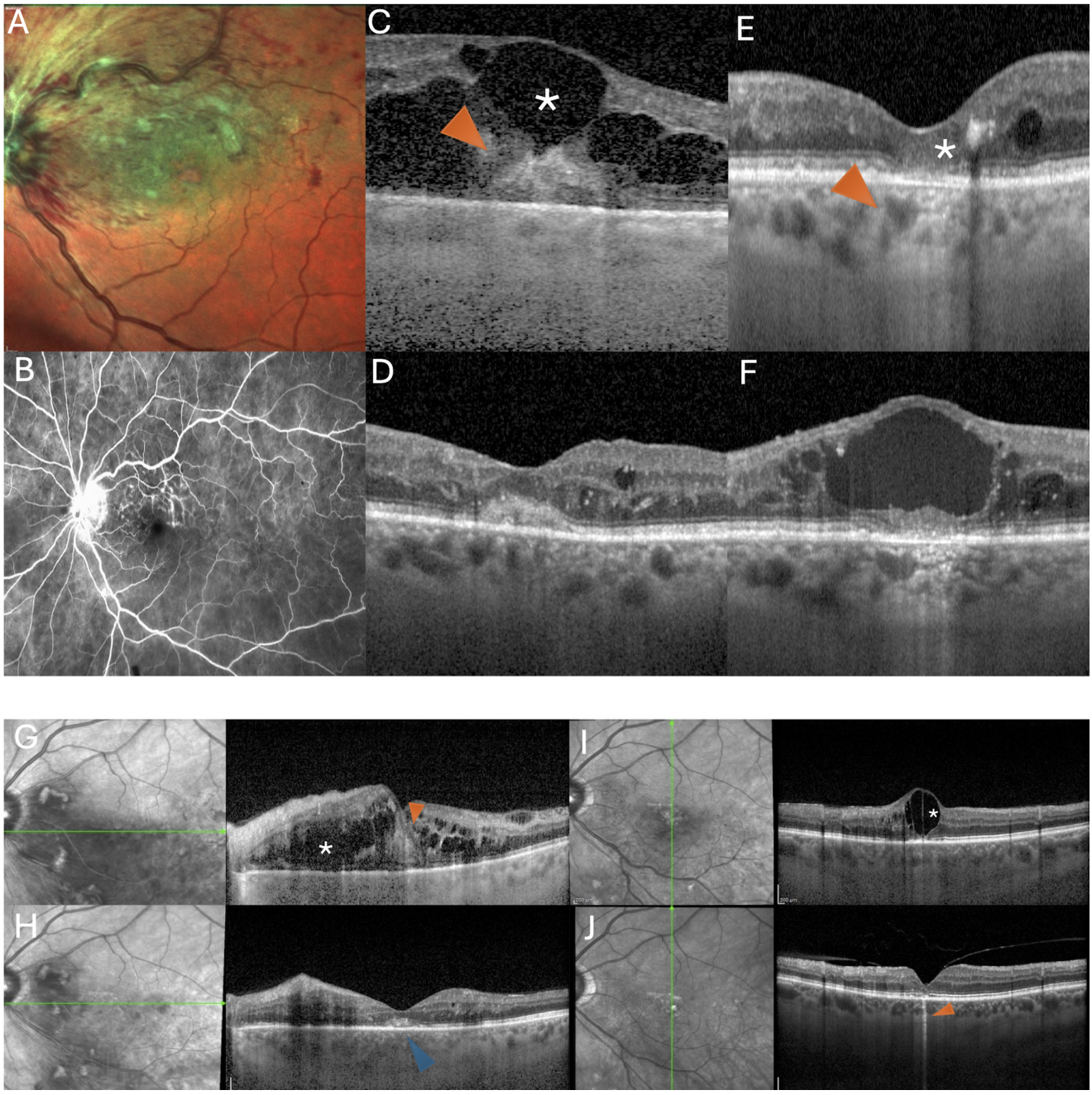

Figure 2. Long-term follow-up of CBH in branch RVO (BRVO), demonstrating progression to outer retinal atrophy. (**A**–**F**) A man in his 70s with superior BRVO. (**A**) Baseline multicolor imaging reveals perifoveal hemorrhages, cotton-wool spots, venous dilation, and foveal cystoid spaces. (**B**) Early-phase FA shows perifoveal hypofluorescence and perivenous leakage. (**C**) OCT demonstrates ONL edema and large cystoid spaces (*white asterisk*) with a vertically oriented hyper-reflective lesion above the ELM (*orange arrowhead*), consistent with CBH. (**D**) At 9 months, OCT shows resolution of edema and a residual hyper-reflective deposit in the outer retina. (**E**) At 8 years, outer retinal atrophy involving the ELM, ellipsoid zone (EZ), and RPE is evident (*orange arrowhead*), along with central DRIL (*white asterisk*). (**F**) At 8.5 years, recurrence of edema presents as a large ONL cyst, indicative of cystoid macular degeneration, with persistent outer retinal atrophy. (**G**–**J**) A man in his 50s with inferior BRVO. (**G**) Baseline OCT reveals intraretinal fluid (*white asterisk*) and a subfoveal piriform hyper-reflective lesion above the ELM (*orange arrowhead*), consistent with CBH. (**H**) At 1 month, OCT shows near-complete fluid resolution and a residual outer retinal hemorrhage (*blue arrowhead*). (**I**) At 8 months, recurrent edema with ONL cysts (*white asterisk*) and focal RPE thickening is observed at the prior CBH site. (**J**) At 3 years, focal central atrophy involving the ELM, EZ, and RPE is evident (*orange arrowhead*).

Investigative Ophthalmology & Visual Science

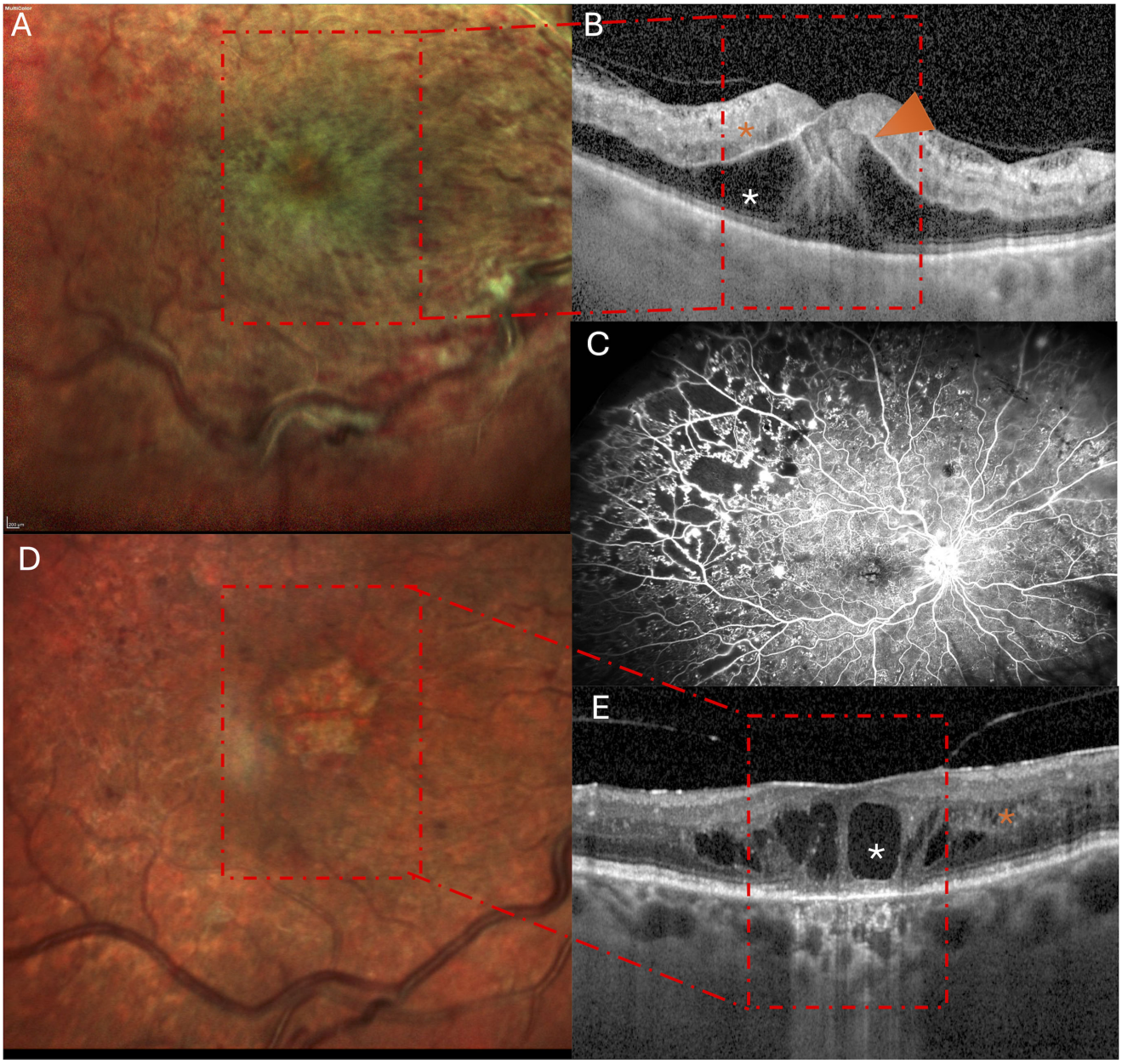

Figure 3. CBH with progression to macular atrophy in CRVO. (**A**) Baseline multicolor imaging reveals diffuse macular thickening, central retinal whitening, and a round foveal hemorrhage. (**B**) OCT demonstrates ONL and inner retinal edema (*white asterisk*), a hyper-reflective lesion above the ELM with vertical projections—hallmark CBH (*orange arrowhead*), and signs of acute ischemic injury. (**C**) Mid-phase FA shows widespread peripheral capillary nonperfusion and neovascular buds. (**D**) At 2 years, multicolor imaging shows a sharply delineated zone of macular atrophy. (**E**) OCT demonstrates DRIL (*orange asterisk*), persistent ONL cysts (*white asterisk*), and atrophy of ELM, EZ, and RPE with choroidal hypertransmission.

A subset of eyes (38%) developed a compact, homogeneous, hyper-reflective deposit in the outer retina beneath the site of CBH. This material was typically positioned atop a flat, irregular thickening of the RPE, resembling a drusenoid detachment. On structural OCT and en face reconstructions, the lesion appeared as a horizontally oriented, plaque-like hyper-reflective structure (Fig. 4). Over time, this deposit regressed or resolved, resulting in focal RPE atrophy (75% of eyes). In these cases, the Bruch's membrane remained intact, and the overlying retina was seen in direct apposition to it, accompanied by marked choroidal hypertransmission.

During the resorption process, hyper-reflective foci frequently emerged within the retina—initially clustered around the subretinal deposit and later migrating into the inner retinal layers (57% of eyes). In advanced stages, some eyes developed signs of retinal degeneration, including DRIL in 42% of eyes, atrophic macular changes in 85%, and severe cystoid macular edema with large, angular cysts in 34%. In five cases (5%), rupture of the cyst roof resulted in the formation of a full-thickness macular hole (Fig. 5).

Effect of CBH on VA

Eyes with CBH had significantly worse presenting VA compared with those without CBH. In multivariable regres-

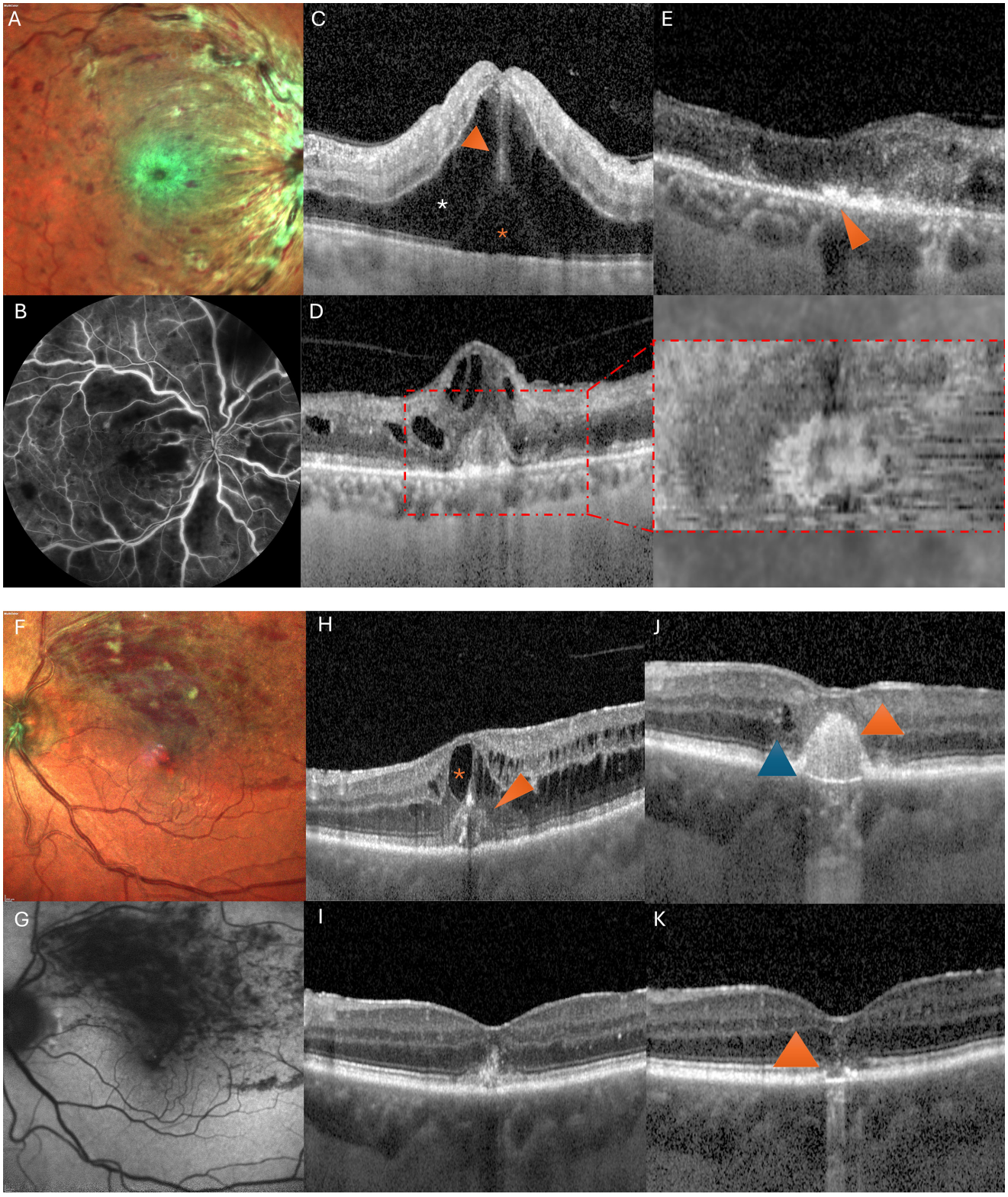

Figure 4. CBH progression to subretinal fibrosis, RPE hyperplasia, and macular atrophy. (**A–E**) A man in his 70s with CRVO. (**A**) Multicolor imaging shows central retinal whitening and foveal hemorrhage. (**B**) FA reveals extensive nonperfusion and enlarged foveal avascular zone. (**C**) OCT shows subretinal fluid (*orange asterisk*), ONL edema (*white asterisk*), and vertically oriented CBH above the ELM (*orange arrowhead*). (**D**) At 2 months, persistent edema and new subfoveal RPE thickening are evident. En face OCT (*red dotted panel*) shows a central plaque-like lesion. (**E**) At 4 months, partial reabsorption of the hyper-reflective lesion, RPE alterations, and EZ disruption indicate progressive atrophy (*orange arrowhead*). (**F–K**) A woman in her 70s with superior branch RVO (BRVO). (**F**) Multicolor imaging reveals perifoveal flame hemorrhages, a central round hemorrhage, and cotton-wool spots. (**G**) Fundus autofluorescence shows central and superotemporal hypoautofluorescence. (**H**) OCT reveals a large ONL cyst (*orange asterisk*), vertically aligned CBH (*orange arrowhead*), and subretinal hemorrhage. (**I**) At 2 months, CBH has partially reabsorbed with residual hyper-reflective material. (**J**) At 6 months, dome-shaped subretinal hyperreflectivity (*orange arrowhead*), RPE atrophy, and fibrosis are evident (*blue arrowhead*). (**K**) At 7 months, outer retinal atrophy with ELM, EZ, and RPE disruption confirms permanent damage (*orange arrowhead*).

Investigative Ophthalmology & Visual Science

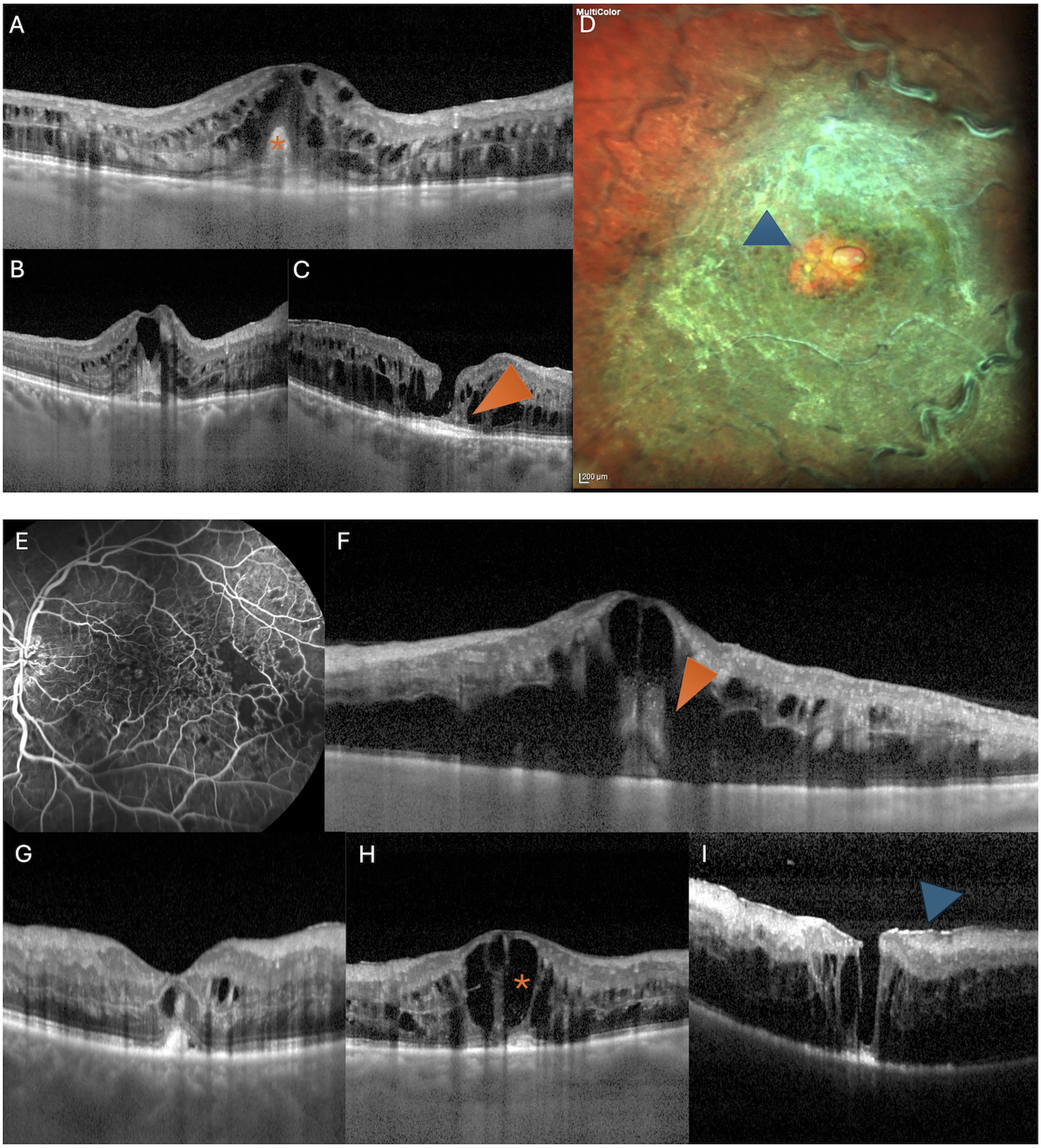

Figure 5. Development of full-thickness macular hole after CBH in CRVO. (**A–D**) A man in his 70s with CRVO. (**A**) Baseline OCT shows ONL edema and piriform CBH above the ELM (*orange asterisk*). (**B**) At 3 months, persistent cysts and early outer retinal disruption are visible. (**C**) At 2 years, OCT reveals a full-thickness macular hole, DRIL, and a persistent subfoveal hyper-reflective plaque (*orange arrowhead*). (**D**) Multicolor imaging confirms central atrophy and open-roof macular hole (*blue arrowhead*). (**E–I**) A man in his 60s with CRVO. (**E**) Early-phase FA shows nonperfusion and central hypofluorescence. (**F**) OCT shows ONL edema, central cysts, and CBH with superior projections (*orange arrowhead*). (**G**) At 1 month, CBH is largely reabsorbed with subretinal hyper-reflective deposit formation. (**H**) At 4 months, recurrent edema, large ONL cysts (*orange asterisk*), and ongoing tissue remodeling are evident. (**I**) At 1 year, OCT reveals a full-thickness macular hole, diffuse cystoid degeneration, and epiretinal membrane (*blue arrowhead*). This case exemplifies the long-term degenerative consequences of CBH.

Table 2. Multivariable Linear Regression of Variable Associated With Presenting VA (logMAR)

Variable	Estimate (β)	95% CI	*P* Value
CBH	0.09	0.00 to 0.18	0.04*
Age (per 10 years)	0.06	0.04 to 0.08	<0.001*
CMT (per 100 µm)	0.07	0.05 to 0.08	<0.001*
RNFL edema	0.12	0.02 to 0.23	0.02*
RNFL hyper-reflectivity	0.07	−0.02 to 0.15	0.1
PAMM arteriolar	0.43	0.28 to 0.58	<0.001*
p-MLM sign	0.06	−0.02 to 0.14	0.2

p-MLM, prominent middle limiting membrane; SRF, subretinal fluid.

Model fit: Residual standard error = 0.34; adjusted $R^2 = 0.4625$; $F(7, 395) = 50.41$; $P < 2.2e{-}16$.

Data are presented as beta coefficients with 95% CIs and corresponding p-values.

*P-value < 0.05 was considered statistically significant.

sion, the presence of CBH was independently associated with poorer baseline VA (β = 0.09 logMAR; 95% confidence interval [CI], 0.00–0.18; P = 0.041). Eyes from older patients (per 10-year increase; β = 0.06 logMAR; 95% CI, 0.04–0.08; P < 0.001), with greater CMT (per 100 µm; β = 0.07 logMAR; 95% CI, 0.05–0.08; P < 0.001), RNFL edema (β = 0.12 logMAR; 95% CI, 0.02–0.23; P = 0.017), and arteriolar PAMM lesions (β = 0.43 logMAR; 95% CI, 0.28–0.58; P < 0.001) also showed worse presenting VA. RNFL hyper-reflectivity and the prominent middle limiting membrane sign did not attain statistical significance, but trended toward worse outcomes. The final model accounted for 46% of the variance in VA (adjusted $R^2 = 0.46$) (Table 2).

Over time, eyes with CBH showed a modest improvement in VA (β for CBH × Time = −0.0023 logMAR/month; P < 0.001). However, despite this improvement, they consistently had lower VA compared with non-CBH eyes, which started with better baseline VA and remained largely stable throughout follow-up (Fig. 6A).

Treatment Frequency and Incidence of Macular Atrophy

Among the 111 eyes with CBH, 108 (97%) had a mean duration of longitudinal follow-up of 35.7 ± 31.5 months. Of the 108 eyes with CBH and follow-up, 102 eyes (94%) received intravitreal treatment, and 6 eyes (6%) remained untreated. Among the treated eyes, 55 (54%) received anti-VEGF agents (ranibizumab or aflibercept) as first-line therapy, and 47 eyes (46%) received dexamethasone implants initially. Across the entire follow-up, the mean number of intravitreal injections per treated eye was 9.6 ± 10.0, with a median of 6 injections (range, 1–61 injections). The distribution was right skewed owing to a minority of eyes requiring prolonged therapy.

During the follow-up period, 75 eyes (69%) developed macular atrophy. The cumulative incidence of macular atrophy was 30% at 6 months, 51% at 12 months, and 88% at 36 months, highlighting the high rate of progressive outer retinal degeneration in this subgroup (Fig. 6B). Of these eyes, 102 (94%) received at least one intravitreal injection, and 6 (6%) remained untreated. In a Cox regression model, treated eyes demonstrated a significantly lower hazard of developing macular atrophy compared with untreated eyes (HR, 0.28; 95% CI, 0.08–0.96; P = 0.04). Additionally, a greater number of injections was associated with a lower risk of macular atrophy (HR per injection, 0.96; 95% CI, 0.93–0.99; P = 0.02), suggesting a protective effect of ongoing therapy. In contrast, the choice of first-line treatment (HR, 0.95 dexamethasone vs. anti-VEGF agents; 95% CI, 0.58–1.54; P = 0.8) and the days elapsed between CBH diagnosis and first injection (median, 17 days; interquartile range, 6–31 days; HR, 0.88 per day; 95% CI, 0.41–1.31; P = 0.7) did not significantly affect the risk of macular atrophy.

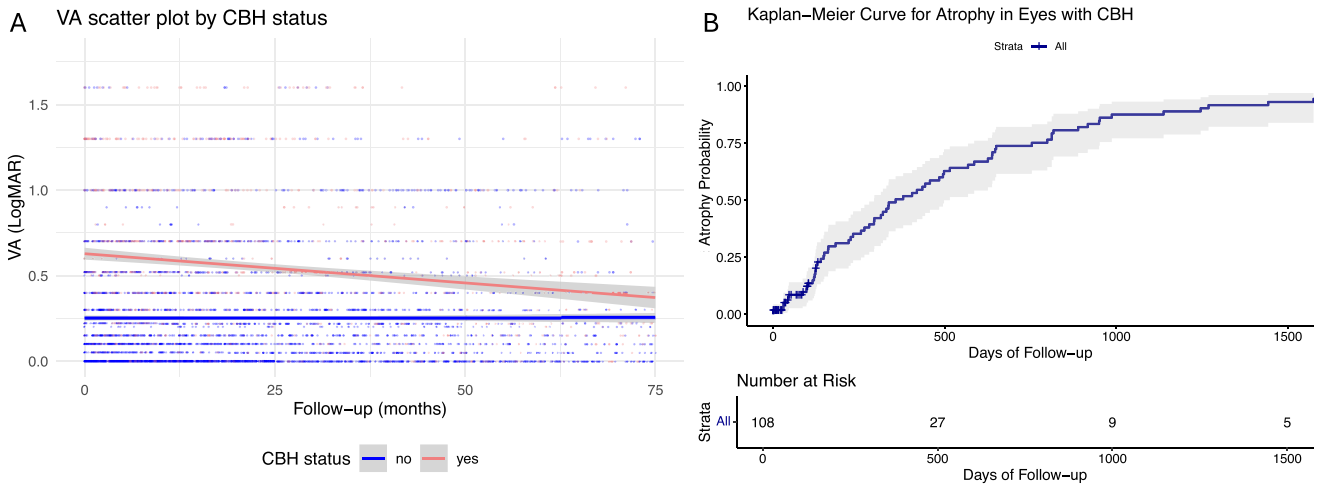

Figure 6. Visual and anatomical outcomes in eyes with CBH. (**A**) Longitudinal scatterplot showing best-corrected VA (logMAR) as a function of time from diagnosis (in months) in eyes with CBH (*red*) and without CBH (*blue*). Each dot represents a visit-level VA measurement. Smoothed regression lines with 95% CIs (*shaded areas*) illustrate trends in VA over time. Eyes with CBH started with significantly worse baseline VA and demonstrated a modest but significant improvement during follow-up. However, their functional outcomes remained inferior to eyes without CBH, which showed more stable and better-preserved vision throughout the study period. (**B**) Kaplan–Meier survival curve showing the cumulative probability of RPE atrophy in 108 eyes with CBH over time. The *x* axis represents days of follow-up; the *y* axis indicates the estimated probability of atrophy development. Numbers below the graph show the number of eyes at risk at each time interval. This analysis highlights the progressive nature of RPE damage in CBH eyes, with a steep increase in incidence within the first 3 years.

Investigative Ophthalmology & Visual Science

Discussion

In this large cohort of treatment-naïve eyes with RVO, CBH was a relatively common and clinically relevant finding, observed in more than one-quarter of cases. CBH was a marker of disease severity, associated with advanced age, a greater prevalence of systemic vascular comorbidities, more severe macular edema, and significantly worse visual and structural outcomes. Affected eyes exhibited a greater frequency of hemorrhagic and ischemic features on OCT and a markedly higher cumulative incidence of RPE atrophy over time. Although CBH eyes showed partial visual improvement during follow-up, their functional prognosis consistently lagged behind that of non-CBH eyes.

The clinical importance of retinal hemorrhages in RVO has long been recognized. Hayreh and Zimmerman[18] demonstrated that severe hemorrhages were more prevalent in ischemic compared with nonischemic CRVO, highlighting the association between hemorrhagic severity and retinal ischemia. Subsequent studies using ultra-widefield angiography confirmed that retinal hemorrhages, particularly those arising from the DCP, are strongly associated with nonperfusion areas.[19] Au et al.[4] proposed a mechanistic model in which hemorrhages initiate in the DCP and propagate centrifugally through progressively more superficial plexuses, mirroring the cascade of venous pressure elevation and ischemic damage. Within this framework, CBH can be viewed as a focal manifestation of severe macular involvement, characterized by a consistent anatomical location, distinctive morphology, and a strong association with outer retinal damage. Its presence complements other hemorrhagic signs and may serve as a useful indicator of disease severity and risk of progressive retinal degeneration in RVO.

Among hemorrhagic manifestations, those involving the macula are especially prevalent and visually detrimental. In SCORE2 (Study of Comparative Treatments for Retinal Vein Occlusion 2), macular hemorrhages were found in more than 95% of treatment-naïve RVO eyes, with nearly 88% showing hemorrhages within the central subfield.[20] Powers et al.[11] similarly reported that 19% of branch RVO cases presented with fovea-involving intraretinal hemorrhages, which were associated with worse baseline VA, greater macular thickness, and a higher prevalence of cystoid macular edema. Despite receiving more frequent anti-VEGF treatments, these eyes demonstrated inferior visual outcomes and persistent edema, suggesting that central macular hemorrhage may be a surrogate marker of deeper ischemic injury and potential treatment resistance. However, whereas Powers et al. highlighted the prognostic implications of foveal hemorrhage, they did not describe their specific structural morphology. Our study expands on this work by introducing and characterizing CBH as a distinctive OCT sign with unique imaging features and clinical trajectory, part of a pattern of severe morphological changes in RVO.

CBH is defined by the accumulation of blood within the central foveal cone bouquet and the associated Müller cell cone—an anatomically and functionally specialized glial scaffold essential for foveal integrity.[10] This microanatomical niche plays an important role in retinal structure, metabolism, and homeostasis. Disruption of this complex, as occurs with CBH, disorganizes both glial and neuronal elements; as the hemorrhage resolves, persistent structural damage—including DRIL and cystoid degeneration—is commonly observed, reflecting irreversible Müller cell dysfunction. Cone bouquet involvement may contribute to explaining the modest correlation between CMT and VA in macular edema secondary to RVO, as previously noted in SCORE[21] and more recent studies.[22] Our findings also align with data in diabetic macular edema, in which disruption of the Müller cell cone was associated with DRIL, foveal ischemia, and reduced anatomical response to anti-VEGF therapy.[23]

Blood accumulation in the intraretinal and subretinal spaces is highly toxic to retinal tissues. Its breakdown products—particularly iron, hemoglobin, and reactive oxygen species—induce not only direct structural damage, but also trigger a maladaptive wound-healing response.[24] The RPE, exposed to these toxic byproducts, undergoes reactive hypertrophy in an effort to clear debris, resulting in hyperpigmentation, thickening, and cellular migration. Concurrently, chronic inflammation and oxidative stress promote subretinal fibrosis through the transdifferentiation of RPE cells into myofibroblasts, leading to extracellular matrix deposition.[25] These mechanisms are well-established in neovascular AMD, where large hemorrhages correlate with worse outcomes. In CATT (Comparison of Age-related Macular Degeneration Treatments Trials), eyes with greater than 50% lesion blood content had significantly higher rates of foveal scarring at 1 and 2 years,[26] and similar trends were reported by Scupola et al.[27] in eyes with subfoveal hemorrhage of 1 disc diameter or greater. Collectively, these observations underscore that hemorrhage is not merely a marker of disease severity, but also a direct contributor to macular degeneration. Within this framework, CBH in RVO may act through analogous mechanisms, initiating a cascade of RPE stress, fibrosis, and chronic retinal damage that culminates in macular atrophy and visual loss.

In our cohort, subretinal hemorrhage co-occurred with CBH in approximately two-thirds of cases, and this combined presence likely amplified outer retinal injury and accelerated RPE degeneration. Anatomical continuity between CBH and subretinal hemorrhage was observed frequently, suggesting that blood may traverse retinal layers into the subretinal space, thereby compounding photoreceptor and RPE toxicity. The synergistic effects of CBH and subretinal hemorrhage likely contribute to the high incidence of macular atrophy observed in affected eyes.

Intravitreal anti-VEGF agents and corticosteroids are the mainstays of treatment for RVO-associated macular edema.[28] Prior analyses from SCORE[20] showed that anti-VEGF treatment decreased hemorrhagic burden compared with the natural course of the disease, and similar findings were reported in CRUISE and BRAVO (A Study of the Efficacy and Safety of Ranibizumab Injection in Patients With Macular Edema Secondary to Branch Retinal Vein Occlusion),[29] where ranibizumab led to a greater proportion of hemorrhage-free retinas compared with sham treatment. We build on this evidence by demonstrating that sustained intravitreal therapy may also decrease the risk of macular atrophy in CBH. However, the choice between anti-VEGF and dexamethasone as the first-line therapy did not affect outcomes significantly, suggesting that consistent treatment, rather than drug class, was critical in preserving retinal integrity. Notably, the number of days elapsed from CBH diagnosis to the first injection was not associated with the risk of macular atrophy. This lack of association may suggest that CBH-related retinal injury begins early in the disease course and progresses irrespective of timing of initiating therapy. In contrast, it is also possible that the treatment

Investigative Ophthalmology & Visual Science

intervals in our cohort were relatively short and insufficient to detect a time-dependent effect.

This study has limitations. First, its retrospective design is inherently subject to selection bias and limits causal inference. Second, the timing and choice of treatment were not standardized, but rather driven by clinical judgment, introducing heterogeneity in therapeutic exposure. Third, although CBH was identified and characterized using high-resolution OCT, multimodal imaging was not available in all cases, potentially limiting comprehensive phenotyping in some eyes. Fourth, although we identified an association between CBH and worse visual and anatomical outcomes, we cannot exclude the influence of other confounding factors, such as baseline ischemic status or undetected systemic conditions, despite the use of multivariable analysis. Last, the diagnosis of macular atrophy was based on structural OCT changes, without confirmatory functional testing, which may underestimate subtle or early functional impairment.

Conclusions

CBH represents a clinically meaningful form of intraretinal hemorrhage in RVO, characterized by its consistent foveal location and distinctive OCT appearance. Its presence is associated with more severe baseline disease, a greater ischemic burden, and an increased risk of progressive retinal degeneration and poor visual outcomes. Our findings suggest that CBH may contribute to disruption of the central foveal Müller cell scaffold, often leading to persistent inner retinal disorganization and macular atrophy. Early and sustained intravitreal treatment may offer some protection against long-term damage. Although CBH does not represent a separate clinical subtype, it serves as a useful structural biomarker for disease severity and may aid in risk stratification and therapeutic decision-making in RVO-associated macular edema.

Acknowledgments

Declaration of Generative AI Technologies in the Writing Process: During the preparation of this work, the authors used chatGPT4.5 to improve readability and language of the manuscript. After using this tool/service, the authors reviewed and edited the content as needed and took full responsibility for the content of the publication.

Author Contributions: All the authors contributed to the conception or design of the work, the acquisition, analysis, and interpretation of data, drafting of the work, revising it critically for intellectual content. Each of the coauthors has seen and agrees with the way his or her name is listed.

Disclosure: **M. Vittoria Cicinelli**, None; **E.M. Pepe**, None; **P. Ramtohul**, None; **B. Tombolini**, None; **S. Puligheddu**, None; **A. Russo**, None; **F. Bandello**, Allergan Inc (C), Bayer Shering-Pharma (C), Hoffmann-La-Roche (C), Novartis (C), Sanofi-Aventis (C), Thrombogenics (C), Zeiss (C), Boehringer-Ingelheim (C), Fidia Sooft (C), Ntc Pharma (C), and Sifi (C); **R. Lattanzio**, None

References

1. Scott IU, Campochiaro PA, Newman NJ, Biousse V. Retinal vascular occlusions. *Lancet*. 2020;396(10266):1927–1940.
2. Rogers S, McIntosh RL, Cheung N, et al. The prevalence of retinal vein occlusion: pooled data from population studies from the United States, Europe, Asia, and Australia. *Ophthalmology*. 2010;117(2):313–319 e311.
3. Bakhoum MF, Freund KB, Dolz-Marco R, et al. Paracentral acute middle maculopathy and the ischemic cascade associated with retinal vascular occlusion. *Am J Ophthalmol*. 2018;195:143–153.
4. Au A, Hilely A, Scharf J, et al. Relationship between nerve fiber layer hemorrhages and outcomes in central retinal vein occlusion. *Invest Ophthalmol Vis Sci*. 2020;61(5):54.
5. Baumal CR, Sarraf D, Bryant T, et al. Henle fibre layer haemorrhage: clinical features and pathogenesis. *Br J Ophthalmol*. 2021;105(3):374–380.
6. Ramtohul P, Cabral D, Sadda S, et al. The OCT angular sign of Henle fiber layer (HFL) hyperreflectivity (ASHH) and the pathoanatomy of the HFL in macular disease. *Prog Retin Eye Res*. 2023;95:101135.
7. Hendrickson AE, Yuodelis C. The morphological development of the human fovea. *Ophthalmology*. 1984;91(6):603–612.
8. Yamada E. Some structural features of the fovea centralis in the human retina. *Arch Ophthalmol*. 1969;82(2):151–159.
9. Ferri A, Ramtohul P, Russo A, et al. Central bouquet hemorrhages in pathologic myopia: clinical characteristics and prognostic relevance. *Ophthalmol Retina*. 2024;8(9):914–923.
10. Ramtohul P, Au A, Kunkler AL, et al. Central bouquet hemorrhage: clinical and multimodal imaging features. *Retina*. 2024;44(4):551–557.
11. Powers JH, Thomas AS, Mir TA, et al. Impact and implication of fovea-involving intraretinal hemorrhage after acute branch retinal vein occlusion. *Ophthalmol Retina*. 2019;3(9):760–766.
12. Midena E, Torresin T, Schiavon S, et al. The Disorganization of retinal inner layers is correlated to muller cells impairment in diabetic macular edema: an imaging and omics study. *Int J Mol Sci*. 2023;24(11):9607.
13. Sadda SR, Guymer R, Holz FG, et al. Consensus definition for atrophy associated with age-related macular degeneration on OCT: Classification of Atrophy Report 3. *Ophthalmology*. 2018;125(4):537–548.
14. Yu S, Pang CE, Gong Y, et al. The spectrum of superficial and deep capillary ischemia in retinal artery occlusion. *Am J Ophthalmol*. 2015;159(1):53–63 e51–52.
15. Chu YK, Hong YT, Byeon SH, Kwon OW. In vivo detection of acute ischemic damages in retinal arterial occlusion with optical coherence tomography: a "prominent middle limiting membrane sign". *Retina*. 2013;33(10):2110–2117.
16. Sridhar J, Shahlaee A, Rahimy E, et al. Optical coherence tomography angiography and en face optical coherence tomography features of paracentral acute middle maculopathy. *Am J Ophthalmol*. 2015;160(6):1259–1268 e1252.
17. Rabiolo A, Cicinelli MV, Corbelli E, et al. Correlation analysis between foveal avascular zone and peripheral ischemic index in diabetic retinopathy: a pilot study. *Ophthalmol Retina*. 2018;2(1):46–52.
18. Hayreh SS, Zimmerman MB. Fundus changes in central retinal vein occlusion. *Retina*. 2015;35(1):29–42.
19. Tanaka S, Tanaka Y, Inoue T, et al. Retinal haemorrhages on ultra-widefield red channel images and perfusion status in central retinal vein occlusion. *Eye (Lond)*. 2023;37(11):2305–2309.
20. Hendrick A, VanVeldhuisen PC, Scott IU, et al. SCORE2 Report 13: intraretinal hemorrhage changes in eyes with central or hemiretinal vein occlusion managed with aflibercept, bevacizumab or observation. Secondary analysis of the SCORE and SCORE2 clinical trials. *Am J Ophthalmol*. 2021;222:185–193.

21. Scott IU, Oden NL, VanVeldhuisen PC, et al. SCORE2 report 24: nonlinear relationship of retinal thickness and visual acuity in central retinal and hemiretinal vein occlusion. *Ophthalmology*. 2023;130(10):1066–1072.
22. Ciulla TA, Kapik B, Hu A, et al. Anatomic biomarkers of macular edema associated with retinal vein occlusion. *Ophthalmol Retina*. 2022;6(12):1206–1220.
23. Choi M, Yun C, Oh JH, Kim SW. Foveal Muller cell cone as a prognostic optical coherence tomography biomarker for initial response to antivascular endothelial growth factor treatment in cystoid diabetic macular edema. *Retina*. 2022;42(1):129–137.
24. Stanescu-Segall D, Balta F, Jackson TL. Submacular hemorrhage in neovascular age-related macular degeneration: a synthesis of the literature. *Surv Ophthalmol*. 2016;61(1):18–32.
25. Zhao S, Rizzolo LJ, Barnstable CJ. Differentiation and transdifferentiation of the retinal pigment epithelium. *Int Rev Cytol*. 1997;171:225–266.
26. Altaweel MM, Daniel E, Martin DF, et al. Outcomes of eyes with lesions composed of >50% blood in the Comparison of Age-related Macular Degeneration Treatments Trials (CATT). *Ophthalmology*. 2015;122(2):391–398 e395.
27. Scupola A, Coscas G, Soubrane G, Balestrazzi E. Natural history of macular subretinal hemorrhage in age-related macular degeneration. *Ophthalmologica*. 1999;213(2):97–102.
28. Giuffre C, Cicinelli MV, Marchese A, et al. Simultaneous intravitreal dexamethasone and aflibercept for refractory macular edema secondary to retinal vein occlusion. *Graefes Arch Clin Exp Ophthalmol*. 2020;258(4):787–793.
29. Campochiaro PA, Brown DM, Awh CC, et al. Sustained benefits from ranibizumab for macular edema following central retinal vein occlusion: twelve-month outcomes of a phase III study. *Ophthalmology*. 2011;118(10):2041–2049.

Investigative Ophthalmology & Visual Science